

# MODIS EVI AS AN ANCILLARY DATA FOR AN OBJECT-BASED IMAGE ANALYSIS WITH MULTI-SPECTRAL MODIS DATA

Y. Gao<sup>a,\*</sup>, J.F. Mas<sup>a</sup>

<sup>a</sup> Centro de Investigaciones en Geografía Ambiental, Universidad Nacional Autónoma de México (UNAM), Antigua Carretera a Pátzcuaro No. 8701 Col. Ex-Hacienda de San José de La Huerta, C.P. 58190 Morelia, Michoacán, México.  
[gaoyan@igg.unam.mx](mailto:gaoyan@igg.unam.mx), [jfmas@ciga.unam.mx](mailto:jfmas@ciga.unam.mx)

**KEY WORDS:** Enhanced Vegetation Index (EVI), Moderate Resolution Imaging Spectral-radiometer (MODIS), Phenology, Object-based image analysis

## ABSTRACT:

This paper investigates the contribution of Enhanced Vegetation Index (EVI) data to the improvement of object-based image analysis using multi-spectral Moderate Resolution Imaging Spectral-radiometer (MODIS) imagery. Object-based image analysis classifies objects instead of single pixels. The idea to classify objects stems from the fact that most often the important information to process an image is not presented in single pixels but in groups of pixels (objects) (Blaschke *et al.* 2001). Based on image segmentation, object-based image analysis uses not only spectral related information, but spatial, textural and contextual information as well. However, which type of information to use depends on the image data and the application, among many other factors. EVI data are from the MODIS sensor aboard Terra spacecraft. EVI improves upon the quality of Normalized Difference Vegetation Index (NDVI) product. It corrects for some distortions in the reflected light caused by the particles in the air as well as the ground cover below the vegetation. The EVI data product also does not become saturated as easily as NDVI when viewing rainforests and other area of the Earth with large amounts of chlorophyll. In this research, 69 EVI data (scenes) collected during the period of three years (from January of 2001 to December of 2003) in a mountainous vegetated area were used to study the correlation between EVI and the typical green vegetation growth stages. These data sets can also be used to study the phenology of the land cover types. Different land cover types show distinct fluctuations over time in EVI values and this information might be used to improve land cover classification of this area. Object-based image analysis was used to perform the land cover classification: one was only with MODIS multispectral data (seven bands), and the other one included also the 69 EVI images. Eight land cover types were distinguished and they are temperate forest, tropical dry forest, grassland, irrigated agriculture, rain-fed agriculture, orchards, lava flows and human settlement. The two classifications were evaluated with independent (from the training data) verification data, and the results showed that with EVI data, the classification accuracy was significantly improved, at 0.01% level, evaluated by McNemar's test.

## 1. INTRODUCTION

In the last three decades, advances in computer technology, earth observation sensors and GIS science, led to the development of "Object-based image analysis" as an alternative to the traditional pixel-based image analysis. Many studies have shown that traditional pixel-based image analysis is limited because basically it uses only spectral information of single pixels and thus produces poor results especially with high spatial resolution satellite images. By contrast, object-based image analysis (OBIA) works on (homogeneous) objects which are produced by image segmentation. As an object is a group of pixels, its characteristics such as the mean, standard deviation of spectral values, etc. can be calculated and used in the classification; besides shape and texture features of the objects can also be derived and used to differentiate land cover classes with similar spectral information.

Enhanced Vegetation Index (EVI) data were obtained from the MODIS sensor aboard Terra spacecraft. EVI improves upon the quality of NDVI product. It corrects for some distortions in the reflected light caused by the particles in the air as well as the ground cover below the vegetation. The EVI data product also

does not become saturated as easily as NDVI when viewing rainforests and other area of the Earth with large amounts of chlorophyll. The EVI data are designed to provide consistent, spatial and temporal comparisons of vegetation conditions, and it offers the potential for regional analysis and systematic and effective monitoring of the forest area. This paper investigates the contribution of EVI data to the improvement of the performance of OBIA with MODIS imagery. The 69 EVI data collected during the period 2001 to 2003 were plotted to obtain the phenology information of the land cover types.

Phenology is the study of the times of recurring natural phenomena. One of the most successful of these approaches is based on tracking the temporal change of a Vegetation Index such as NDVI or EVI. The evolution of vegetation index exhibits a strong correlation with the typical green vegetation growth stages. The results (temporal curves) can be analyzed to obtain useful information such as the start/end of vegetation growing season. However, remote sensing based phenological analysis results are only an approximation of the true biological growth stages. This is mainly due to the limitation of current space based remote sensing, especially the spatial resolution, and the nature of vegetation index. A pixel in an image does not

---

\* Corresponding author.

contain a pure target but a mixture of whatever intersected the sensor's field of view.

Since EVI is a good indicator of the phenology of the land cover types, the research tested the contribution of EVI data to the land cover classification. OBIA was carried out: one was with single date MODIS spectral reflectance data (seven bands), and the other one included also the EVI data (69 dates). The classification results were evaluated with independent verification data and were compared in order to examine the contribution of the EVI data to image classification using object based method with MODIS multi-spectral data.

## 2. STUDY AREA AND DATA

### 2.1 The study area

The study area is located in Michoacán state, central west of México, covering an area of approximately 58\*60 km<sup>2</sup>, within the longitude of 102° 00' W and 102° 32' W, and latitude of 19° 02' N and 19° 36' N (figure 1). The main land cover types in the study area are temperate forest, tropical dry forest, orchards, grassland, irrigated agriculture, rain fed agriculture, lava flow, and human settlement.

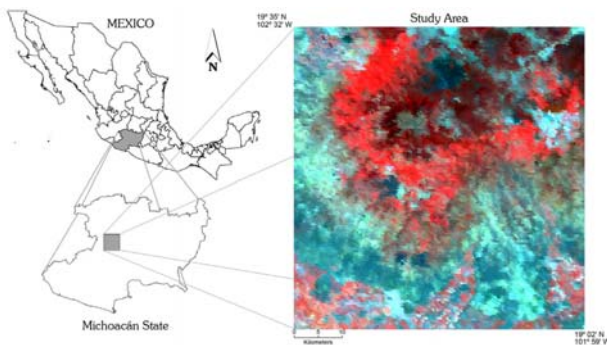


**Figure 1:** The study area. Left side of the figure are two sketch maps indicating México and Michoacán state where the study area is located; right side is the false colour composite of MODIS imagery with R, G, B represented by bands 2 (near-infrared), band 1 (red), and band 3 (green).

### 2.2 Earth observation data

This part of the research relies on the data acquired by the MODIS instrument on board Terra and Aqua satellites from National Aeronautics and Space Administration (NASA). Terra MODIS and Aqua MODIS take between one and two days to cover the entire Earth's surface, with a complete 16-day repeat cycle. Both sensors acquire data in 36 spectral bands, or groups of wavelengths, and their spatial resolution (pixel size at nadir) is 250m for channels 1 and 2 (0.6 µm -0.9 µm), 500m for channels 3 to 7 (0.4 µm -2.1 µm) and 1000m for channels 8 to 36 (0.4 µm -14.4 µm). These channels are calibrated on orbit by a solar diffuser (SD) and a solar diffuser stability monitor (SDSM) system, which convert the Earth surface radiance to radio-metrically and geo-location calibrated products for each band (Xiong *et al.* 2003). Although recent evaluations have reported a geo-location error of 113m at nadir (Knight *et al.* 2006), official technical specifications warrant 50m geo-location accuracy (Wolfe *et al.* 2002). In both cases, the geo-location is less than half a pixel dimension, and hence acceptable for the multi-spectral analysis (Carrao *et al.* 2007).

The data acquired by the MODIS sensor is used to generate multiple products at different pre-process stages. In this study the MOD09A1 product was used, a weekly composite of surface reflectance images, freely available from MODIS Data Product website (<http://modis.gsfc.nasa.gov>). This specific product is an estimate of the surface spectral reflectance imaged at a nominal spatial resolution of 500m for the first seven bands as it would have been measured at ground level if there were no atmospheric scattering or absorption. The applied correction scheme compensates for the effects of gaseous and aerosol scattering and absorption, for adjacency effects caused by variation of land cover, for Bidirectional Reflectance Distribution Function (BRDF), for coupling effects, and for contamination by thin cirrus (Vermote and Vermeulen 1999). Seven first spectral bands (1-7) of MOD09A1 imagery obtained on 08 March 2007 were used because they are closely related to land cover mapping. In addition, a set of 69 MODIS Enhanced Vegetation Index (EVI) images covering a full three years observation period, from January 2001 to December 2003 were also used for image classification.

EVI is an 'optimized' index designed to enhance the vegetation signal with improved sensitivity in high biomass regions and improved vegetation monitoring through a de-coupling of the canopy background signal and a reduction in atmosphere influence. EVI is computed following this equation (Huete *et al.* 2002):

$$EVI = G * \frac{(NIR - Red)}{(NIR + c1 * Red - c2 * Blue + L)}$$

Where NIR/red/blue are atmospherically corrected or partially atmosphere corrected (Rayleigh and ozone absorption) surface reflectance, L is the canopy background adjustment that addresses non-linear, differential NIR and red radiant transfer through a canopy, and c1, c2 are the coefficients of the aerosol resistance term, which uses the blue band to correct for aerosol influence in the red band. The coefficients adopted in the MODIS EVI algorithm are: L = 1, c1 = 6, c2 = 7.5, and G (gain factor) = 2.5. Whereas the NDVI is chlorophyll sensitive, the EVI is more responsive to canopy structural variations, including leaf area index (LAI), canopy type, plant physiognomy, and canopy architecture. The two VIs complement each other in global vegetation studies and improve the detection of vegetation changes and extraction of canopy biophysical parameters. For this work, OBIA is carried out in an object-based image analysis software eCognition (Definiens 2006).

## 3. METHODS

### 3.1 OBIA in eCognition

OBIA in eCognition comprises two parts: multi-resolution image segmentation and classification based on objects' features in spectral, spatial, and textural domains. Image segmentation is a kind of regionalization, which delineates objects according to a certain homogeneity criteria and at the same time requires spatial contingency (Lang *et al.* 2006). Several parameters are used here to guide the segmentation result. The scale parameter determines the maximum allowed heterogeneity for the resulting image objects. The colour criterion defines the weight with which the spectral values of

the image layers contributes to image segmentation, as opposed to the weight of the shape criterion. The relationship between colour and shape criteria is: colour + shape = 1. Maximum colour criterion 1.0 results in objects spectrally homogeneous; while with a value of less than 0.1, the created objects would not be related to the spectral information at all. Smoothness is used to optimize image objects with regard to smooth borders, and compactness allows optimizing image objects with regard to compactness (Batz *et al.* 2004). The resulting objects also depend on the image data. For a given set of segmentation parameters, heterogeneous image data result in smaller image objects than homogeneous image data.

The image objects can then be classified either using a (standard) nearest neighbour (NN) classifier or fuzzy membership function, or a combination of both. The first classifier describes the class by user-defined sample objects, while the second one describes intervals of feature characteristics (Hofmann 2001b). The variety of object features can be used either to describe fuzzy membership functions, or to determine the feature space for NN. More detailed description of image segmentation and classification is given in Hofmann (2001a) and Gao *et al.* (2006). In this paper, the OBIA was performed with a standard NN classifier.

### 3.2 Accuracy assessment

Classification accuracy is used to describe the degree to which the derived image classification agrees with reality (Campbell 1996), and a classification error is, thus, the discrepancy between thematic map and reality. Accuracy assessment result is often represented by a confusion matrix. It is a simple cross-tabulation of the mapped class label against that observed one in the ground or reference data for a sample of cases at specified locations. The confusion matrix provides an obvious foundation for accuracy assessment (Campbell 1996, Canters 1997), by providing the basis to both describe classification accuracy and characterize errors, which may help to refine the classification. Many measures of classification accuracy can be derived from a confusion matrix (Stehman 1997). One of the most popular is the percentage of cases correctly allocated which is often regarded as *overall accuracy*, which is calculated by dividing the total number of the verification data with the number of the correctly classified image data. For the accuracy of individual classes, the percentage of cases correctly allocated may be derived from the confusion matrix by relating the number of cases correctly allocated to the class to the total number of cases of that class. This can be achieved from two standpoints, depending on whether the calculations are based on the matrix's row (*user's accuracy*) or column marginal (*producer's accuracy*) (Foody 2002). The detailed description of the error matrix and the calculation of the measures of classification accuracy can be found in the second chapter 2.4.

Image classifications were evaluated with independent reference data which comprised of in total 496 points. These points were generated with a stratified random sampling method. Based on the land use map from the year 2000, random points were extracted from the 8 classes of interest. The properties of these points were interpreted based on the information from ortho-corrected photographs (1995), land use map from year 2000, and Landsat-7 ETM+ image (2003).

### 3.3 The test of McNemar

Map accuracy statements are often compared to evaluate the relative suitability of different classification techniques for mapping. Accuracy statements should be compared in a statistically rigorous fashion to provide a more objective basis for comment and interpretation (Foody 2004). In many remote sensing studies, the same set of ground data are used in the assessment of the accuracy of the thematic maps to be compared. For related samples, the statistical significance of the difference between two accuracy statements maybe evaluated using tests that take into account the lack of independence such as McNemar's test. It is a non-parametric test that is based on confusion matrixes that are 2 by 2 in dimension. The attention is focused on the binary distinction between correct and incorrect class allocations. The McNemar test equation can be expressed as

$$Z^2 = \frac{(f_{12} - f_{21})^2}{f_{12} + f_{21}}$$

In which  $f_{ij}$  indicates the frequency of verification samples lying in confusion matrix element  $i$  and  $j$ .  $f_{12}$  and  $f_{21}$  are the number of pixels that with one method were correctly classified, while with the other one were incorrectly classified.  $Z^2$  follows a chi-squared distribution with one degree of freedom (Agresti 1996). The statistical significance can be obtained with the derived  $z^2$  compared against tabulated chi-square values. For example, with one degree of freedom, when the calculated  $z^2 \geq 3.84$ , the two classifications are significantly different at 0.05% level; when  $z^2 \geq 6.64$ , the two classifications are significantly different at 0.01% level; when  $z^2 \geq 10.83$ , the two classification are significantly different at 0.001% level; and when  $z^2 < 3.84$ , the two classifications are not significantly different.

## 4. RESULTS

### 4.1. Phenology of land cover types

69 EVI images from 2001 to 2003 were used to monitor the phenology of the eight land cover types.

In figure 6-2, the horizontal axis represents the 69 MODIS EVI data in three years from which, each year there are 23 image data. The vertical axis represents the EVI values of the land cover types from different time of the year. The 23 images from each year were taken every 16 days. In the example of the image data from 2001, roughly, image data 1 and 2 corresponds to data from January, 3 and 4 corresponds to February, and so on and so forth. The figure shows that for land cover types such as 'rain fed agriculture', 'tropical dry forest' and 'grassland', there are big changes in EVI values during different seasons in the period of three years; while for 'lava flow' and 'human settlement' the fluctuation of the EVI values during different seasons of the year is small. In the example of EVI values of 'tropical dry forest', the EVI values are low for image data 1 to 11, which corresponds in season to January – the end of May, dry season in México. In dry season, 'tropical dry forest' loses all the leaves and becomes totally dry, causing the rather low EVI values during this period. Its EVI values start to rise from data 11 and reach its peak on 17/18, which corresponds to the period from the end of May to the end of September and which is the rainy season in Mexico. Thus 'tropical dry forest' has high EVI values because in rainy season it regains its leaves

and tends to have higher reflection in near infrared band. From data 18 its EVI value starts to drop and keeps dropping until data 28 which corresponds to March/April of the next year, during which the dry season starts and continues until the beginning of the rainy season of the next year. 'Tropical dry forest' and 'grassland' show evident seasonal change of EVI data because the growth of these two land cover types depends on the water from the natural rain. Other land cover types such as 'lava flow' and 'human settlement', having few vegetation cover, do not show much change in EVI values during different seasons of the year. Also, their EVI values are rather low among the eight land cover types (the EVI value of 'human settlement' is even lower than that of the 'tropical dry forest' during the dry season due to little vegetation cover). Figure 6-2 also shows that during the dry season, four land cover types 'grassland', 'human settlement', 'rain fed agriculture', and 'tropical dry forest' are not separable.

Land cover types such as 'orchard', 'irrigated agriculture', and 'temperate forest' show high EVI values during the year and small fluctuations during different seasons of the year. These land cover types keep green all the year round and show only small difference between dry season and rainy season. The sudden drop of the EVI value of data 11 for 'orchards' is due to the noise of image data. In rainy season, the constant presence of rain clouds influences the image data quality and produce noises. One way to derive the missing value at this point is to average data value 10 and 12.

#### **4.2. OBIA with single data MODIS multispectral imagery**

First, the multispectral MODIS image was segmented using the following parameters: scale factor 20, colour 0.7, shape 0.3, and smoothness 0.5. By giving more weights to colour factor, the segmentation procedure considers more spectral information. For the shape factor, we gave the same weight to smoothness and compactness for the produced objects. The selection of the parameters was based on the visual checking. Altogether 3518 objects were created. In the class hierarchy, eight land cover classes were created and for each of them, the standard nearest neighbour classifier using the mean values of the spectral information from the 7 bands of MODIS multispectral image. Training samples were defined for each of the seven classes, and the image was classified (figure 6-4). The classified image was evaluated with the independent verification data which is comprised of 499 stratified random sample points. Error matrix was produced and it is shown in table 6-1. The classification obtained an overall accuracy 57.3%.

#### **4.3. OBIA with multi-date EVI data and multispectral imagery**

OBIA was performed with both single date spectral reflectance data and 69 dates EVI data. Image was segmented with only 7 spectral reflectance bands and with the same parameters in order to obtain the same number of objects as the first classification (section 6.4.3). The same class hierarchy and the same training samples were used for the eight classes of interest. NN classifier was also used here but based not only on the spectral information of the reflectance data, but also on the 69 EVI data. The image was classified and shown in figures 6-5. In the obtained result, land cover types were visually more homogeneous. The classified image was evaluated with the same independent reference data which is comprised of 499 stratified random sample points. Error matrix was produced and

it is shown in table 6-2. This classification obtained an overall accuracy 62.5%.

#### **4.4. Comparison and discussion**

The two classifications were compared. The OBIA using both single date spectral reflectance data and multiple dates EVI data shows an improvement of 5.2% in accuracy than that obtained by using only single date spectral reflectance data. McNemar's test was used to evaluate the significance of the difference between these two classifications. 249 pixels were correctly classified and 150 pixels were wrongly classified by both classifications, 63 pixels were correctly classified by the classification with both spectral reflectance and EVI data, and 37 pixels were correctly classified by the classification using only spectral reflectance data. The calculated chi-square  $Z^2 = 6.76$ . Checked by the significance table, the two classifications are significantly different, at 0.01% level. The result shows that the OBIA with both spectral reflectance and EVI data obtained the accuracy significantly higher than the classification with only spectral reflectance data. Further checking these two classifications shows that the improvement is mainly represented by classes 'tropical dry forest', 'lava flow', 'orchards', and 'irrigated agriculture', which contributed 3.8%, 0.8%, 1.0%, and 2.2% to the improvement of the accuracy, respectively. As shown in the accuracy assessment tables, by adding the EVI data, the spectral confusion between 'tropical dry forest' and 'rain fed agriculture' in the MODIS image was alleviated and it improved 15.4% the produced accuracy of 'tropical dry forest'. EVI data alleviated the confusion between 'lava flow' and 'tropical dry forest'; between 'irrigated agriculture', and 'grassland'; and between 'orchards' and 'irrigated agriculture'.

The MODIS spectral reflectance data contain information from visible, near infrared and mid infrared spectral regions which record the most important spectral signature of the classes for land cover mapping. Due to the coarse spatial resolution of 250m and 500m, multi-spectral MODIS image was composed mostly of mixed pixels, which reduced the spectral separability between classes of interest. The multi-date EVI data helped to separate land cover classes which were difficult to be differentiated with only single date spectral reflectance information. For example the 'grassland' showed serious spectral confusion with 'rain fed agriculture' in the spectral reflectance image; also 'tropical dry forest' and 'lava flow'; and 'rain fed agriculture' and 'tropical dry forest'. By observing figure 6-2, we can see that these pairs of classes exhibit different reflectance values and are separable using EVI data.

### **5. CONCLUSIONS**

This research investigates the contribution of EVI data to the improvement of OBIA with MODIS spectral reflectance data. The evolution of the 69 EVI data collected during the period 2001 to 2003 exhibits a strong correlation with the phenology of the land cover types. The results (temporal curves) were analyzed and various land cover types show different fluctuations in EVI values, which were used to improve the land cover classification. OBIA was carried out for land cover classification: one was only with MODIS spectral reflectance data, and the other one included also the 69 EVI images. The classifications were evaluated with independent verification

data, and the results showed that with EVI data, the accuracy was significantly improved, at a level of 0.01%, by McNemar's test. This paper shows that the MODIS EVI data supply important information not only to monitor the phenology of the land cover types, but to differentiate land cover types which were difficult to be differentiated using single date spectral reflectance data.

#### ACKNOWLEDGEMENT

The authors thank CONACYT-CONAFOR 2005-C02-14741 for supplying PhD fellowship to the first author during writing up of the paper.

#### References

- Baatz, M., and Schaepe, A., 1999. Object-oriented and multi-scale image analysis in semantic networks. 2<sup>nd</sup> International Symposium: Operationalization of Remote Sensing, 16-20 August, ITC, the Netherlands.
- Baatz, M., Benz, U., Dehghani, S., Heynen, M., Holtje, A., Hofmann, P., Lingenfelder, I., Mimler, M., Sohlbach, M., Weber, M., Willhauck, G., 2004, eCognition User's Guide. <http://www2.definiens.com/central/default.asp> (the last accessed 07/March/2006).
- Bastin, L., 1997, Comparison of fuzzy c-means classification, linear mixture modeling and MLC probabilities as tools for unmixing coarse pixels. *International Journal of Remote Sensing*, 18, pp. 3629-3648.
- Blaschke, T., and Strobl, J., 2001, What's wrong with pixels? Some recent development interfacing remote sensing and GIS. *GeoBIT/GIS*, 6, pp. 12-17.
- Campbell, J.B., 1996, *Introduction to Remote Sensing* (2<sup>nd</sup> ed.). London: Taylor and Francis.
- Canters, F., 1997, Evaluating the uncertainty of area estimates derived from fuzzy land-cover classification. *Photogrammetric Engineering and Remote Sensing*, 63, pp. 403-414.
- Carrao, H., Goncalves, P., Caetano, M., 2007, Contribution of multispectral and multitemporal information from MODIS images to land cover classification. *Remote Sensing of Environment*, doi: 10.1016/j.rse.2007.07.002.
- Dean, A.M., Smith, G.M., 2003, An evaluation of per-parcel land cover mapping using maximum likelihood class probabilities. *International Journal of Remote Sensing*, 24, pp. 2905-2920.
- Definiens, 2006. *Definiens professional User Guide 5*. Definiens AG, Munich.
- Foody, G.M., 2002, Status of land cover classification accuracy assessment. *Remote sensing of environment*, 80, pp. 185-201.
- Gao, Y., Mas, J. F., Maathuis, B. H. P., Zhang, X. M., and Van Dijk, P. M., 2006. Comparison of pixel-based and object-oriented image classification approaches-a case study in a coal fire area, Wuda, Inner Mongolia, China. *International Journal of Remote Sensing*, 27, pp. 4039-4051.
- Hay, G.J., and Gastilla, G., 2006, Object-based image analysis: strength, weakness, opportunities, and threats (SWOT). 1<sup>st</sup> International Conference on Object-based image analysis (OBIA 2006), 4-5, July, 2006, Salzburg, Austria.
- Hofmann, P. 2001a. Detecting buildings and roads from IKONOS data using additional elevation information. In: *GeoBIT/GIS* 6, pp. 28-33.
- Hofmann, P., 2001b. Detecting urban features from IKONOS data using an object-oriented approach. In: *Remote Sensing & Photogrammetry Society (Editor): Proceedings of the First Annual Conference of the Remote Sensing & Photogrammetry Society 2001*, pp. 28-33.
- Huete, A., Didan, K., Miura, T., Rodriguez, E.P., Gao, X., Ferreira, L.G., 2002, Overview of the radiometric and biophysical performance of the MODIS vegetation indices. *Remote Sensing of Environment*, 83, pp. 195-213.
- Integrated Land and Water Information System (ILWIS), 2005. *International Institute for Geo-Information Science and Earth Observation (ITC)*. The Netherlands
- Justice, C.O., Markham, B.L., Townshend, J.R.G., and Kennard, R.L., 1989, Spatial degradation of satellite data. *International Journal of Remote Sensing*, 10, pp. 1539-1561.
- Lillesand, M., Kiefer, W.R., 1994, *Remote sensing and image interpretation*, Third Edition, John Wiley & Sons, Inc., New York, 750 pp.
- Smits, P.C., Dellepiane, S.G., Schowengerdt, R.A., 1999, Quality assessment of image classification algorithms for land-cover mapping: a review and proposal for a cost-based approach. *International Journal of Remote Sensing*, 20, pp.1461-1486.
- Stehman, S.V., 1997, Selecting and interpreting measures of thematic classification accuracy. *Remote sensing of Environment*, 62, pp. 77-89.
- Vermote, E.F., Vermeulen, A., 1999, atmospheric correction algorithm: Spectral reflectances (MOD09) algorithm technical background document. Available online at [http://modis.gsfc.nasa.gov/data/atbd/atbd\\_mod08.pdf](http://modis.gsfc.nasa.gov/data/atbd/atbd_mod08.pdf) (accessed 16 December 2007).
- Wolfe, R.E., Nishihama, M., Fleig, A.J., Kuyper, J.A., Roy, D.P., Storey, J.C., Patt, F.S., 2002, Achieving sub-pixel geolocation accuracy in support of MODIS land science. *Remote Sensing of Environment*, 83, pp. 31-49.
- Xiong, X., Sun, J., Esposito, J., Guenther, B., & Barnes, W.L., 2003, MODIS reflective solar bands calibration algorithm and on-orbit performance. *Proceedings of SPIE-Optical Remote Sensing of the Atmosphere and Clouds III*, Vol. 4891, pp. 95-104.